Theoretical Investigation of the Dimerization of Linear Alkenes Catalyzed by Acidic Zeolites

Stian Svelle,*,† Stein Kolboe,† and Ole Swang‡

Department of Chemistry, University of Oslo, P.O. Box 1033 Blindern, N-0315 Oslo, Norway, and SINTEF Applied Chemistry, Department of Hydrocarbon Process Chemistry, P.O. Box 124 Blindern, N-0134 Oslo, Norway

Received: October 22, 2003; In Final Form: December 19, 2003

The zeolite-catalyzed dimerization of ethene, propene, 1-butene, and *trans*-2-butene has been modeled using quantum chemical methods. Reactants, transition states, and products have been investigated. A cluster model consisting of four tetrahedrally coordinated atoms (T-atoms) has been used to represent the catalyst. Two different mechanism types have been evaluated: concerted and stepwise. In the concerted pathway, protonation and C−C bond formation occur simultaneously. The stepwise mechanism proceeds via alkoxide formation followed by C−C bond formation. The order of reactivity among the different alkene reactants has been assessed. Quantum chemistry predicts that the activation energy of the concerted mechanism lies between the two barriers of the stepwise mechanism. More detailed knowledge concerning the stability of alkoxide species relative to physisorbed alkenes will be necessary for discrimination between the two mechanistic proposals. Implications for the reverse reaction, the β-scission of alkenes, are briefly discussed.

1. Introduction

Dimerization and oligomerization of lower alkenes to form higher molecular weight products may be an attractive route for the production of high octane number gasoline.[1] In particular, the dimerization of butenes has become increasingly interesting because methyl *tert*-butyl ether (MTBE), a well-known high octane oxygenate blending component, is required to be replaced by environmentally more beneficial alternatives.[2] The traditional catalyst for propene and butene oligomerization is phosphoric acid impregnated on a solid kieselguhr carrier, known as the solid phosphoric acid (SPA) catalyst.[3] The SPA catalyst displays excellent activity and selectivity. However, safely disposing of the spent catalyst, which contains organic tars and is highly acidic, is challenging. Regenerable zeolites have been investigated as alternatives and been found to be well suited as catalysts for alkene dimerization and oligomerization.[4−9] Depending on reaction conditions, the products may be in the gasoline range,[8] but lubricants can also be manufactured.[5]

Apart from these practical applications, zeolite-catalyzed alkene dimerization is also interesting from a more fundamental viewpoint, as alkene dimerization is an elementary reaction which may occur in many zeolite-catalyzed hydrocarbon transformations. In particular, during the conversion of methanol to hydrocarbons (MTH), the concentration of alkenes escaping the zeolite pore systems can be quite high.[10] It is therefore of interest to evaluate the reactivity of these alkenes with quantum chemical methods. We have previously investigated the reaction of alkenes with a methanol molecule,[11] and in this report we study the combination of two alkene molecules. Increased insight in mechanistic details relevant to the MTH reaction was the original motivation behind the present work.

Dimerization of ethene, propene, 1-butene, and *trans*-2-butene has been investigated. Two different mechanism types, stepwise and concerted, have been explored. The stepwise mechanism proceeds via the initial formation of alkoxides as intermediates, which subsequently react further to form a new C−C bond. The concerted mechanism involves simultaneous protonation and C−C bond formation. Very little theoretical data focusing on the dimerization reaction can be found in the literature. The reverse reaction, alkene β-scission, has been investigated to a limited extent,[12−16] and only via mechanisms involving alkoxide intermediates. The concerted dimerization mechanism presented here appears to be novel. It has been of primary interest to compare the reactivity of the various alkenes submitted to calculation and also to efficiently compare the two mechanisms for alkene dimerization. Attempts were made also to investigate the dimerization of 2-methylpropene (iso-butene), but it was not possible to model this reaction via the mechanisms outlined above. Rather, attempts to find transition states gave *tert*-butyl carbenium ions as energy minima, as described also by Sinclair et al.[17] in a QM/MM-study. There have been no experimental observations of simple alkyl carbenium ions in zeolites, and these computational results might be artifacts. Also, two iso-butene molecules are considerably bulkier than the other pairs of reactants, and we speculate that the limit to the usefulness of our cluster model (see below) has been reached or transcended in the iso-butene case. It therefore seems that the iso-butene reaction requires substantial further investigations, beyond the scope of the present work, before a satisfactory description may be given.

A 19-atom cluster model containing four tetrahedral atoms (denoted 4T) has been used to represent the zeolite catalyst. Within the cluster approach, a small fragment is used to simulate the Brønsted acidic site. Calculations with such clusters have proven them to be adequate for qualitative descriptions of chemical rearrangements that occur locally on the active site.[16] Structure-specific effects and effects caused by the electrostatic field present in the zeolite micropores are, however, not well described. The same cluster as employed in this work has been used by several workers to model reactions similar to those

* Corresponding author. E-mail: stian.svelle@kjemi.uio.no.
† University of Oslo.
‡ SINTEF Applied Chemistry.

10.1021/jp0371985 CCC: $27.50
Published on Web 02/10/2004

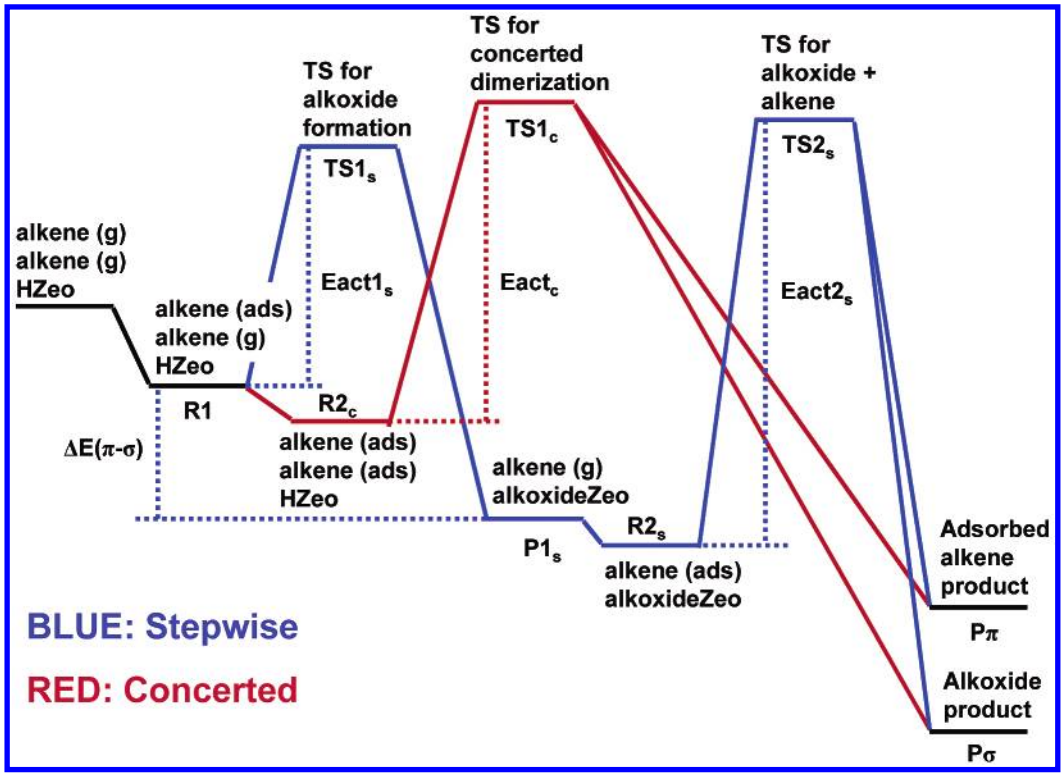

Figure 1. Energy profiles of the concerted and stepwise dimerization mechanisms.

described here: Methylation of alkenes[11] and methylbenzenes[18] by methanol and halomethanes[19] and also the ethylation and iso-propylation of methylbenzenes[20] have been investigated. Moreover, Rozanska et al.[21,22] studied the isomerization and transalkylation of toluene and xylenes and found that the relative order of the activation energies is conserved when comparing results obtained when using the same cluster as here with calculations relying on periodic boundary conditions (zeolite mordenite) combined with plane wave basis sets.

2. Computational Details

All calculations were done using the Gaussian98 program package.[23] The B3LYP hybrid density functional combined with 6-31G(d) basis sets were employed for all geometry optimizations. No geometric constraints were used in the optimizations. The ultrafine integration grid was used in order to ensure convergence. Additionally, single-point electronic energies were calculated for the optimized geometries using B3LYP and MP2 combined with larger, triple-ζ basis sets with polarization functions on all atoms. These schemes are denoted B3LYP/cc-pVTZ//B3LYP/6-31G(d) and MP2/6-311G(d,p)//B3LYP/6-31G(d).

The zeolite catalyst has been modeled by a widely used cluster consisting of four tetrahedral atoms, i.e., three silicon and one aluminum atom to generate the acidic site.[18] For most stationary points, there is more than one possible orientation of the reactant relative to the cluster. These possibilities are usually indistinguishable in energy, but care has been taken to select stationary points in which reactants and products were coordinated similarly to the cluster for all reactions. This makes comparisons for trends easier, but should otherwise not influence the results. For all stationary points, vibrational spectra were calculated to ensure that the correct number of imaginary frequencies was at hand, i.e., one imaginary frequency for transition states and zero for energy minima. For the transition states, the normal modes corresponding to the imaginary frequencies were visualized to confirm that they indeed corresponded to the expected motion of atoms. Internal reaction coordinate (IRC) calculations, as implemented in Gaussian98, were in some cases carried out. Such calculations follow reaction paths in both directions from a given transition state in order to investigate the minima connected by the transition state. A stepsize of 0.3 $amu^{-1/2}$ bohr and the ultrafine integration grid were used. The transition states were also investigated by perturbing the geometries very slightly along the reaction coordinate corresponding to the negative eigenvalue in the Hessian, and using the geometries thus produced as starting points for energy minimizations. This quasi-IRC approach occasionally yields information not readily derived from strictly rigorous IRC-calculations. In combination, these two techniques did confirm that the transition states found involve the rupture and formation of the required bonds, thus properly describing the desired reactions. In the following, when energies are discussed, we refer to the B3LYP/6-31G(d) + ZPE values, unless otherwise stated.

3. Results and Discussion

Dimerization of ethene, propene, 1-butene, and *trans*-2-butene has been submitted to quantum chemical analysis. Two different mechanisms have been evaluated, a stepwise pathway (subsection 3.1) and a concerted mechanism (subsection 3.2). Figure 1 displays the energy profiles of both mechanisms and labels the stationary points described in the following discussion. These labels will be used for comparison of the potential energy surfaces (PES) of the two mechanisms. All transition states explored are carbenium ion-like. For the concerted mechanism, we investigated the formation of primary, as well as secondary, carbenium ion-like species in the transition states. For the stepwise mechanism, only the intuitively most stable possibilities were analyzed. As the reactions proceed along the reaction coordinate from the dimerization transition states toward the products, (at least) two possibilities can be envisaged: immediate deprotonation to yield a neutral alkene or formation of an alkoxide species. Both possibilities have been investigated and the corresponding energies are reported. These aspects are dis-

TABLE 1: Products Investigated for the Various Dimerization Reactions

reactant	alkoxide[a]	alkene product
ethene	1-butoxide	1-butene
propene (s)[b]	4-methyl-2-pentoxide	4-methyl-2-pentene
propene (p)[c]	2-hexoxide	2-hexene
1-butene (s)	5-methyl-3-heptoxide	5-methyl-3-heptene
1-butene (p)	3-octoxide	3-octene
trans-2-butene	3,4-dimethyl-2-hexoxide	3,4-dimethyl-2-hexene

[a] The last number designates the carbon atom bonded to the zeolite oxygen. Branches are considered as substituents on a linear carbon chain. [b] (s) = formally secondary carbenium ion in the transition state. [c] (p) = formally primary carbenium ion in the transition state.

cussed thoroughly in the following sections. For most reactions, deprotonation immediately after the transition state could result in several different alkenes. In these cases, the thermodynamically most stable products were selected. Possible hydride- or methyl-shifts were not considered. Table 1 lists the products formed in the investigated reactions.

Implications for the reverse reaction, the β-scission, are discussed briefly in subsection 3.4.

3.1. Stepwise Dimerization. In this pathway, one alkene molecule is initially adsorbed on the cluster, and an alkoxide species is formed. Subsequently, a second alkene is adsorbed onto the cluster with the alkoxide group, and in the second step the alkoxide leaves the zeolite wall and a C−C bond is formed. Figure 2 shows the stationary points for the formation of ethoxide from ethene, and Figure 3 displays the reaction of the ethoxide group with the second ethene molecule. Energies for the stepwise mechanism are listed in Table 2. Geometric parameters for alkoxide formation and the further reaction are listed in Tables 3 and 4, respectively.

The formation of alkoxide species (σ-complex) from alkenes coordinated to the zeolite acidic site (as π-complex), or alkene chemisorption, has been the subject of numerous previous theoretical investigations.[17,24−31] Our results are in general accord with the bulk of previously published data and will be discussed in brevity. In the transition state for alkoxide

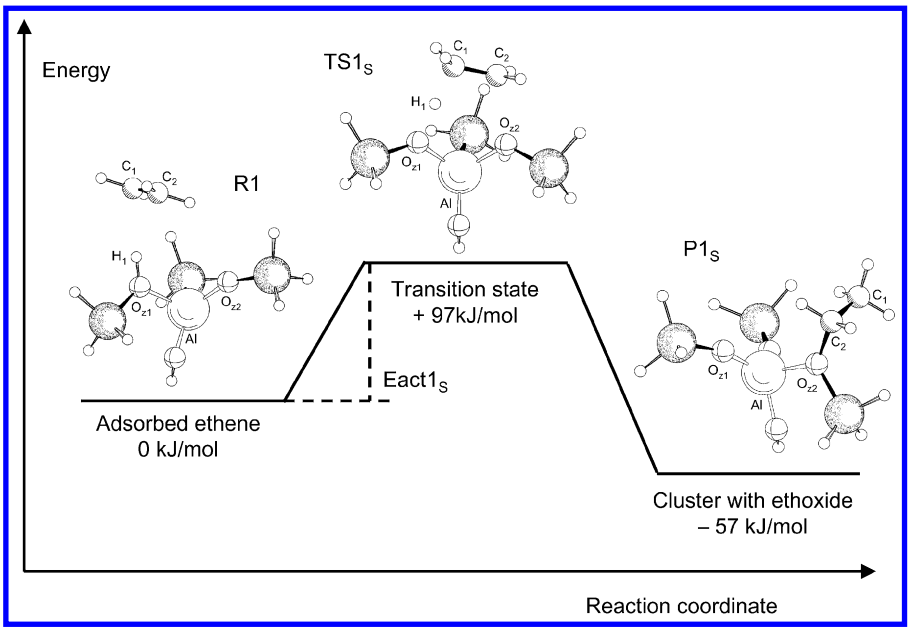

Figure 2. Stationary points for formation of ethoxide group from ethene.

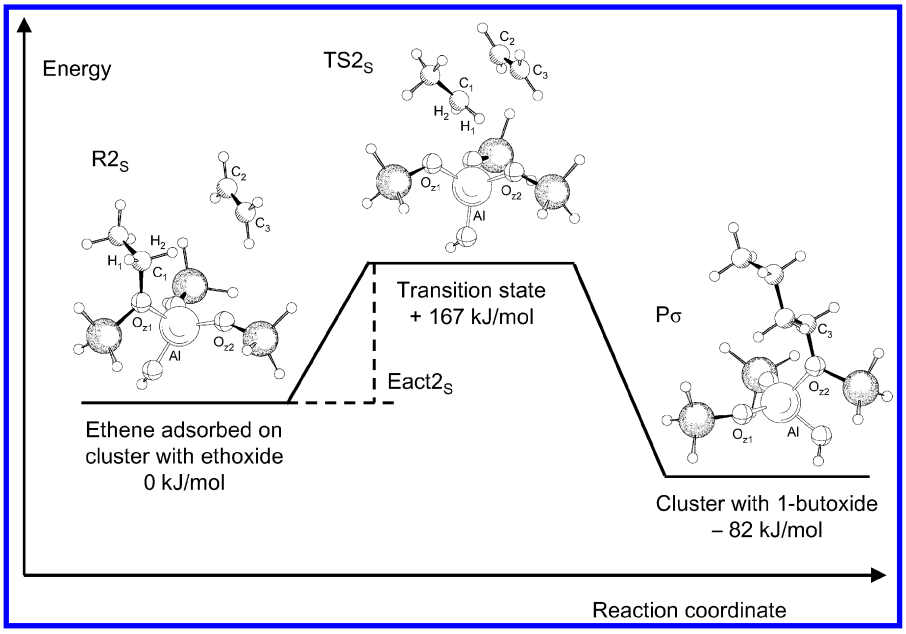

Figure 3. Stationary points for the coupling of an ethoxide group with ethene.

TABLE 2: Energy Parameters for Stepwise Dimerization[a]

	Energy of[b]									
	R1	$TS1_S$	$P1_S$	$R2_S$	$TS2_S$	P_σ	P_π	$\Delta E(\pi\text{-}\sigma)$	$Eact1_S$	$Eact2_S$
					B3LYP/6-31G(d) +ZPE					
ethene	−31	+66	−88	−92	+76	−174	−139	−57	+97	+167
propene	−34	+48	−81	−86	+57	−150	−122	−46	+82	+143
1-butene	−35	+45	−80	−84	+53	−137	−120	−45	+79	+137
trans-2-butene	−34	+61	−63	−66	+72	−91	−94	−29	+96	+139
					B3LYP/6-31G(d)					
ethene	−36	+70	−107	−113	+61	−208	−161	−70	+106	+175
propene	−39	+54	−97	−104	+49	−180	−141	−57	+93	+153
1-butene	−39	+53	−95	−102	+46	−166	−139	−56	+93	+148
trans-2-butene	−39	+66	−80	−85	+66	−123	−113	−40	+105	+151
					B3LYP/cc-pVTZ//B3LYP/6-31G(d)					
ethene	−27	+94	−65	−66	+100	−146	−130	−38	+122	+167
propene	−30	+77	−57	−59	+87	−121	−109	−27	+107	+145
1-butene	−30	+78	−55	−55	+84	−105	−106	−25	+108	+139
trans-2-butene	−29	+89	−41	−40	+99	−64	−82	−12	+118	+140
					MP2/6-311G(d,p)//B3LYP/6-31G(d)					
ethene	−38	+99	−91	−107	+80	−210	−179	−53	+137	+187
propene	−45	+82	−93	−113	+62	−211	−181	−48	+127	+174
1-butene	−47	+81	−93	−115	+50	−202	−181	−46	+128	+165
trans-2-butene	−49	+89	−82	−105	+63	−181	−172	−33	+139	+168

[a] Labels defined in Figure 1; energies in kJ/mol. [b] Relative to two gas-phase alkene reactants and the cluster at infinite separation.

TABLE 3: Geometric Parameters for Formation of Alkoxide Groups[a]

	ethene	propene	1-butene	*trans*-2-butene
adsorbed reactants				
$O_{z1}H_1$	0.98	0.99	0.99	0.99
H_1C_1	2.29	2.14	2.15	2.19
H_1C_2	2.25	2.31	2.30	2.21
C_1C_2	1.34	1.34	1.34	1.34
transition states				
$O_{z1}H_1$	1.34	1.42	1.42	1.48
H_1C_1	1.30	1.25	1.25	1.23
C_1C_2	1.40	1.40	1.41	1.41
$O_{z2}C_2$	2.18	2.37	2.39	2.40
$O_{z1}H_1C_1$	174	176	176	176
dihedral-C_2[b]	176	176	176	177

[a] Atom labels defined in Figure 2; distances in Å, angles in degrees. [b] This is the dihedral angles formed by C_2 and the three substituents on this carbon, indicating the deviation from planarity (180°) around the carbon formally bearing the positive charge in the transition state.

TABLE 4: Geometric Parameters for the Coupling of an Alkoxide Group with an Alkene[a]

	ethene	propene	1-butene	*trans*-2-butene
adsorbed reactants				
$O_{z1}C_1$	1.47	1.49	1.49	1.49
$O_{z2}H_1$	4.23	2.82	2.73	2.72
$O_{z3}H_2$	3.65			
C_1C_2[b]	4.11	4.00	4.07	4.49
C_1C_3[b]	3.95	3.98	4.50	4.12
C_2C_3	1.33	1.34	1.34	1.34
AlC_2	4.55	5.02	5.24	5.39
AlC_3	4.96	4.68	5.37	5.29
$O_{z1}C_2C_3C_1$	136	140	142	142
transition states				
$O_{z1}C_1$	2.36	2.53	2.58	2.67
$O_{z2}H_1$	2.23	2.09	2.09	2.09
$O_{z3}H_2$	2.28			
C_1C_2	2.36	2.59	2.55	2.77
C_1C_3	2.33	2.78	2.75	2.70
C_2C_3	1.35	1.35	1.35	1.35
AlC_2	4.62	5.33	5.35	6.39
AlC_3	4.40	4.66	4.69	4.76
$C_1H_1O_{z2}$	134	163	165	164
$C_1H_2O_{z3}$	138			
$O_{z1}C_2C_3C_1$	165	178	178	177

[a] Atom labels defined in Figure 3; distances in Å, angles in degrees. [b] For propene/1-butene the methyl/ethyl group is attached to C_2.

formation, the acidic proton is about halfway between the zeolite oxygen atom and the alkene carbon atom. Simultaneously, the other carbon atom of the alkene double bond is moving closer to another zeolite oxygen atom, as the C−O bond of the alkoxide is forming. As can be seen from Table 3, going from ethene to propene/1-butene to *trans*-2-butene results in the acidic proton being farther from the zeolite oxygen in the transition state and closer to the alkene carbon, i.e., the proton transfer is gradually more pronounced in this order. Linked to this, the $O_{z2}C_2$ distances become longer as the degree of proton transfer increases. A combination of steric effects and the varying stabilities of the carbenium ion-like transition states upon increased methyl group substitution on the alkene double bond appears to be a reasonable explanation for these trends. The double bond is slightly stretched in the transition state.

The activation barrier decreases by about 15 kJ/mol when going from ethene to propene, which is expected on the basis of the stability of a formally primary carbenium ion (from ethene) compared with a secondary ion (from propene). No significant stabilizing effect can be observed by replacing a methyl group with an ethyl group: the barrier for propene chemisorption is effectively the same as for 1-butene. In fact, the calculated barrier becomes minutely higher for 1-butene when higher-level computational schemes are used. The barrier for alkoxide formation from *trans*-2-butene is markedly higher than for propene and 1-butene, it is actually quite close to that of ethene. This was somewhat unexpected, but agrees quite well with the work of Correa et al.,[25] in which the barrier for *trans*-2-butene chemisorption is reported to be 13 kJ/mol higher than that found for 1-butene. It seems plausible that this predicted reduction in reactivity for *trans*-2-butene compared to 1-butene is caused by steric limitations, because, on the basis of inductive effect argumentation, *trans*-2-butene is expected to be equally or slightly more reactive than propene and 1-butene. The trends in the calculated barriers are reproduced by all computational schemes, although considerable shifts in the energies are found when comparing different methods. For instance, the MP2/

6-311G(d,p)//B3LYP/6-31G(d) approach yields activation energies that are close to 30 kJ/mol higher that those found when using B3LYP/6-31G(d) electronic energies.

The geometries of the formed alkoxides are considered trivial, and no geometric data for these species are listed in Table 3 (see Supporting Information for details). The chemisorption reactions are all found to be quite exothermic, more so for ethene than for propene and 1-butene (for which the energies are equal) than for *trans*-2-butene. Again, the results differ considerably from one method to another. Interestingly, adding the B3LYP/6-31G(d) ZPE correction to the B3LYP/cc-pVTZ//B3LYP/6-31G(d) electronic energy predicts a thermoneutral reaction energy for *trans*-2-butene chemisorption. These reaction energies are of importance with respect to the comparison of the two mechanistic proposals, and will be further elaborated in subsection 3.3.

Further progress of the stepwise mechanism requires the physisorption of a second alkene to the cluster on which an alkoxide group is already formed. In the stationary points thus found, the second alkene is located next to the alkoxide group, interacting with the cluster as well as the alkoxide itself. The adsorption energy is built up from a sum of weak van der Waals forces acting between adsorbate and adsorbent. As is evident when comparing the $P1_S$ (cluster with alkoxide) energies with the $R2_S$ (cluster with alkoxide plus second alkene) energies listed in Table 2, the adsorption energies are poorly predicted by all DFT schemes employed. Typically, the values are in the range 0−5 kJ/mol. More realistic values were found when MP2/6-311G(d,p)//B3LYP/6-31G(d) was used. This shortcoming of DFT methods in describing weak interactions of this kind is well-known.[32]

The next step along the reaction coordinate of the stepwise mechanism is the transition state that describes the formation of the new C−C bond. The $O_{z1}C_1$ bond, which connects the alkoxide with the cluster, is gradually stretched, and at the same time C_1 approaches the alkene double bond. For propene and 1-butene, where the alkene double bond is unsymmetrically substituted, C_1 is becoming connected to least substituted carbon (denoted C_2). Formally, this places the charge on the most substituted carbon (denoted C_3). The C_1C_2 distances are about 0.2 Å longer than the C_1C_3 distances. For ethene and *trans*-2-butene, these distances are more similar, and C_1 evidently approaches the center of the double bond. This ensures that the charge formally is evenly distributed between the equivalent carbon atoms C_2 and C_3 in the transition states. The $O_{z1}C_2C_3C_1$ dihedral angles are close to 180°, indicating that the four atoms lie in the same plane. An exception was found for ethene dimerization, for which the angle was 165°. However, the transition state for ethene dimerization is slightly different from that of the other reactions, as there are two hydrogens on C_1 that form hydrogen bonds with zeolitic oxygen atoms. This is indicated by the $O_{z2}H_1$ and $O_{z3}H_3$ distances listed in Table 4, and might be the cause of the difference. There is a steady increase in the $O_{z1}C_1$ distances in the order ethene < propene < 1-butene < *trans*-2-butene. The distances from C_1 to the alkene double bond also tend to increase in the same order, except that the values found for propene and 1-butene are nearly identical. These trends are probably the result of steric requirements, rather than one transition state being earlier or later than another; there is simply an elongation of the key distances of the transition states as the alkenes become larger.

Activation energies for the step in which the new C−C bond is formed ($Eact2_S$) are listed in data column 10 in Table 2. Ethene dimerization results in the highest barrier. Propene is predicted to be considerably more reactive; the barrier is 24 kJ/mol lower than for ethene. The barriers for 1-butene and *trans*-2-butene are insignificantly different; both lying slightly below that found for propene. This trend is reproduced at every level of theory employed. All barriers are considerably higher than those found for the first step of this mechanism, the chemisorption. Notably, they are in the same range as the barriers for the reverse of the chemisorption, i.e., the release of the alkoxides as physisorbed alkenes.

The transition states described above are similar to the one described by Hay et al.[12] in a study of pentene β-scission, relying on a 3T cluster and HF/6-31G(d) optimizations. Their study corresponds to the combination of an ethoxide with a propene molecule. An activation energy of +188 kJ/mol (HF/6-31G(d) + ZPE) or +163 kJ/mol (B3LYP/6-31G(d)//HF/6-31G(d) + ZPE) can be derived for the ethoxide/propene coupling step. Hay et al.[12] found $O_{z1}C_1$ and C_1C_2 distances about 0.04 Å longer than those found here. Other workers describe similar transition states for alkene β-scission, always relying on less advanced descriptions of the catalyst acidic site compared to those employed in the present study.[13−16]

As mentioned above, there are several possibilities for the progress of the reaction after the transition state in which the C−C bond is formed. Direct deprotonation will lead to a physisorbed alkene product, whereas coordination of the charged carbon atom to a zeolite oxygen will lead to the formation of an alkoxide. This issue was investigated by employing the IRC and quasi-IRC approaches described in Section 2. The rigorous IRC procedure gave limited information, as these calculations terminated after only a modest shift in geometry beyond that of the transition state. All transition states through which C−C bonds are formed were therefore submitted to the quasi-IRC procedure. For most cases, this resulted in direct deprotonation and alkene formation. Three exceptions were found, however: For ethene dimerization, via both mechanisms, and for the stepwise dimerization of *trans*-2-butene, deprotonation leading to the formation of cyclopropane derivatives was observed (see discussion below). Evidently, the outcome of these calculations, i.e., formation of alkenes, cyclopropanes, or alkoxides, is very sensitive to the exact positioning of the methyl groups and other alkyl substituents on the alkenes in the transition states. For example, during the dimerization of 1-butene, an ethyl group might be directed either toward or away from the cluster, resulting in two geometrically different transition states indistinguishable in energy. Such a difference in substituent orientation might possibly lead to a different site of deprotonation or preferred formation of an alkoxide or even a cyclopropane derivative. It is not feasible to explore every possible such orientation. We therefore opted to investigate as products species known to exist in the zeolite pores during such hydrocarbon transformations, i.e., alkoxides and alkenes. The thermodynamically most stable possibilities, not involving hydride- or methyl shifts, were selected (Table 1).

Frash et al.[13] also considered the formation of cyclopropane derivatives, which later on undergo a ring-opening step leading to an alkoxide (for the case of β-scission). However, they could only find cyclopropane derivatives on the PES when B3LYP/6-31G(d) was used for optimizations; these species were not involved when HF/6-31G(d) was employed. Thus, the prediction of cyclopropanes as intermediates was suspected to be a computational artifact.[13] On the basis of the data reported by Frash et al.,[13] a transition state for the ring-opening of methylcyclopropane to form 1-butoxide was optimized, and a fairly high barrier of 151 kJ/mol was found for this step (159

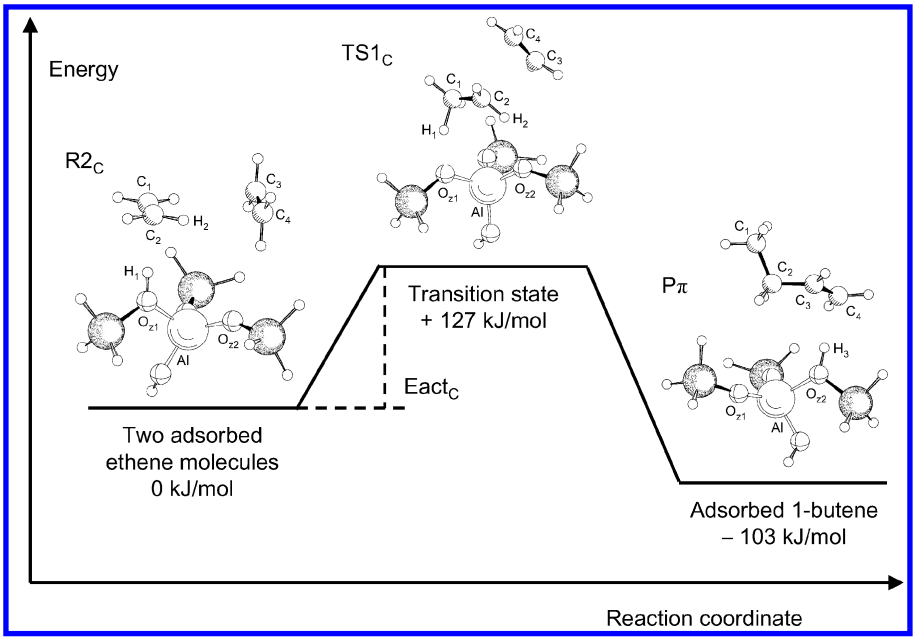

Figure 4. Stationary points for concerted dimerization of two ethene molecules.

kJ/mol without ZPE correction, 167 kJ/mol at the B3LYP/cc-pVTZ//B3LYP/6-31G(d) level, and 203 kJ/mol at the MP2/6-311G(d,p)//B3LYP/6-31G(d) level of theory). We did not succeed in finding a transition state directly connecting methylcyclopropane and 1-butene. The calculated activation energies for the ring-opening are higher than the barrier for concerted ethene dimerization at every level of theory (see below) and also higher than the highest barrier of the stepwise mechanism at the B3LYP/cc-pVTZ//B3LYP/6-31G(d) and the MP2/6-311G(d,p)//B3LYP/6-31G(d) levels of theory. On the basis of this, the detection of cyclopropanes should be facile during experimental studies of alkene dimerization, because of the large ring-opening barrier. We have not been able to find any experimental reports describing extensive formation of cyclopropanes during alkene dimerization/oligomerization, and it is tempting to conclude that their theoretically predicted formation is indeed a computational artifact or that the cluster approach grossly overestimates the ring-opening barrier. If this last possibility were the case, cyclopropanes might very well be short-lived intermediates during alkene dimerization and β-scission.

The above discussion on product formation also applies to the concerted mechanism, and it is thus a matter purely of convenience that the alkoxide is depicted as the product in Figure 3 and the physisorbed alkene is the product in Figure 4 (see below). Details on the geometries of both the π- and σ-coordinated products can be found in the Supporting Information.

All reactions are quite strongly exothermic, and the formation of an alkoxide is energetically more favorable than formation of a π-coordinated alkene. There are, however, a few exceptions to this. In particular, for 3,4-dimethyl-2-hexene formed after dimerization of *trans*-2-butene, the physisorbed alkene lies lower in energy than the alkoxide at the B3LYP/6-31G(d) + ZPE and B3LYP/cc-pVTZ// B3LYP/6-31G(d) levels of theory. This appears to be a trend in the sense that increasing the bulk of the hydrocarbon fragment favors the physisorbed species relative to the alkoxide. It should be noted, however, that as the size of the hydrocarbon increases, the shortcomings of the cluster approach become more pronounced. In particular, some unphysical interactions between the hydrocarbon fragments and the terminating $-SiH_3$ groups cannot be completely avoided. Also, the omission of the surrounding pore structure, and thus also steric constraints, might allow the largest alkoxides and alkenes to adopt unreasonably favorable positions.

3.2. Concerted Dimerization. In the concerted mechanism, protonation and C−C bond formation occur simultaneously in a single step. This is shown in Figure 4, and the energetic and geometric specifics of this pathway are listed in Tables 5 and 6, respectively. The starting point is identical to that of the stepwise mechanism. One alkene is physisorbed onto the acidic site in the previously described side-on manner. Then, rather than forming an alkoxide, a second alkene is physisorbed next to the first, on a siliceous part of the zeolite. The adsorption energy of this second alkene is very small and not well described by DFT methods. Reasonable results are obtained only when MP2 is used, quite analogous to what was found above when an alkene was adsorbed on a cluster with an alkoxide group already attached. At the MP2/6-311G(d,p)//B3LYP/6-31G(d) level of theory, there is a small increase in the adsorption energies in the order of the size of the alkenes.

In the transition state for concerted dimerization, the acidic proton is partially transferred from a zeolite oxygen atom to one of the carbon atoms of the originally π-coordinated alkene. Simultaneously, the other carbon of the double bond is attacked by the π-electrons of the second alkene, resulting in the formation of the new C−C bond. For the unsymmetrically substituted alkenes, there are two possible sites of protonation, leading to formation of either a formally primary or secondary carbenium ion in the transition state. Both options were explored. The reactions proceeding via formally primary ions are best discussed separately from those involving secondary ions, before a comparison is made between the two possibilities.

For ethene, propene, and 1-butene, the concerted mechanism may proceed via transition states involving species resembling primary carbenium ions. As indicated by the $O_{z1}H_1$ and H_1C_1 distances listed in Table 6, the degree of proton transfer from the zeolite to the alkene is greater for ethene dimerization than for propene and 1-butene, which are almost equal in this respect. Also, the distance from C_2, which formally bears the positive charge, to the second alkene double bond is smaller for ethene than for propene/1-butene. It seems that the progress of reaction is greater at the transition state for ethene than for propene and

TABLE 5: Energy Parameters for Concerted Dimerization[a]

	Energy of[b]					
	R1	$R2_C$	TS_C	P_σ	P_π	$Eact_C$
B3LYP/6-31G(d) +ZPE						
ethene	−31	−35	+91	−174	−139	+127
propene (s)	−34	−39	+58	−150	−122	+97
propene (p)			+83	−148	−123	+122
1-butene (s)	−35	−40	+62	−137	−120	+102
1-butene (p)			+81	−140	−125	+120
trans-2-butene	−34	−38	+76	−91	−94	+114
B3LYP/6-31G(d)						
ethene	−36	−44	+87	−208	−161	+131
propene (s)	−39	−47	+58	−180	−141	+105
propene (p)			+82	−179	−143	+129
1-butene (s)	−39	−47	+58	−166	−139	+105
1-butene (p)			+82	−170	−144	+129
trans-2-butene	−39	−45	+71	−123	−113	+116
B3LYP/cc-pVTZ//B3LYP/6-31G(d)						
ethene	−27	−28	+121	−146	−130	+149
propene (s)	−30	−31	+90	−121	−109	+121
propene (p)			+115	−120	−112	+146
1-butene (s)	−30	−30	+94	−105	−106	+124
1-butene (p)			+115	−109	−112	+145
trans-2-butene	−29	−29	+105	−64	−81	+134
MP2/6-311G(d,p)//B3LYP/6-31G(d)						
ethene	−38	−52	+113	−210	−179	+165
propene (s)	−45	−59	+74	−211	−181	+133
propene (p)			+90	−204	−174	+150
1-butene (s)	−47	−65	+75	−202	−181	+140
1-butene (p)			+86	−197	−176	+152
trans-2-butene	−49	−67	+70	−180	−172	+137

[a] Labels defined in Figure 1; energies in kJ/mol. [b] Relative to two gas-phase alkene reactants and the cluster at infinite separation.

1-butene. The highest activation barrier is found for ethene dimerization, and this is especially pronounced when MP2/6-311G(d,p)//B3LYP/6-31G(d) methodology is used. The barriers found for propene and 1-butene are basically identical. This is consistent with the observed variations in the key distances in the transition states described above. A large part of the activation energy is associated with the removal of the acidic proton from the cluster,[11] which is most pronounced in the ethene transition state, thereby raising the barrier. Also, the short C_2C_3 and C_2C_4 distances found for ethene implies greater charge localization on C_2, further enhancing the relative instability of the transition state. The Mulliken charges on C_2 are +0.31e for ethene and +0.26e for propene and 1-butene, thus confirming this notion.

Transition states involving formally secondary carbenium ions are possible for propene, 1-butene, and *trans*-2-butene. Again, trends in geometric and energetic details can be found. When inspecting the activation barriers obtained at the various levels of theory, it seems that the barrier for propene is slightly lower or possibly equal to that found for 1-butene, whereas *trans*-2-butene is predicted to have the lowest reactivity. Thus, the bulk of the results indicate the following order of reactivity in this case: propene ≥ 1-butene > *trans*-2-butene. This somewhat unexpected result is opposite of the order found above when primary carbenium ions were involved as transition states. The degree of proton transfer from the zeolite, indicated by the $O_{z1}H_1$ distance, increases when going from propene to 1-butene to *trans*-2-butene. Also, the C_1C_3 and C_1C_4 distances (C_1 now bears the positive charge) decrease in the same order. As before, it seems that a high activation barrier is coupled with a late transition state. Interestingly, the Mulliken charges on C_1 are +0.32e for propene, +0.31e for 1-butene, and +0.29e for *trans*-2-butene, indicating that the charge delocalization in the transition state is greatest for *trans*-2-butene, which is the intuitive result. One feasible explanation for the unexpectedly low activity of *trans*-2-butene relative to propene/1-butene lies in the reaction energies, which are considerably less exothermic for *trans*-2-butene than for propene and 1-butene, both when the π- and σ-complexes are considered. According to the Brønsted-Polanyi relation,[33] a less exothermic reaction should result in a higher barrier, which is exactly what is found here. Also, steric limitations in the transition state raising the energy cannot be excluded.

For propene and 1-butene protonation leading to both primary and secondary carbenium ion-like transition states is possible, and as very much expected, the secondary option is clearly preferred, by 20−30 kJ/mol. A difference in barrier of 25 kJ/mol corresponds to a factor of 150 in relative reaction rates at 600 K, signaling that protonation at the most favored site is nearly completely dominant. The degree of proton transfer in the transition states is always greater for the secondary alternatives, and this is also reflected in the more severely stretched alkene double bonds (the C_1C_2 distances) for these options. The double bond of the other alkene (C_3C_4) is only moderately stretched in every instance. Some features found in the transition states of the concerted mechanism are independent of the site of protonation. The most noteworthy aspect is the anti-periplanar geometry, most commonly found for E2 elimination reactions. Indeed, when considering the dimerization in the reverse direction, i.e., alkene cracking, the reaction is rightfully labeled as an E2 reaction. The anionic zeolite cluster serves as the base, taking the H_1 proton from the alkene. Simultaneously, the second alkene is lost as a leaving group on the other side of the forming double bond. The geometry around the carbon atom from which the leaving group is lost is nearly planar, as indicated by the dihedral angles listed in Table 6. Another aspect worth pointing out is the nearly isosceles triangular arrangement of the carbon atom formally bearing the positive charge and the two carbons

TABLE 6: Geometric Parameters for Concerted Dimerization[a]

	Primary[b]			Secondary[c]		
	ethene	propene	1-butene	propene	1-butene	*trans*-2-butene
adsorbed reactants						
$O_{z1}H_1$	0.98	0.99	0.99			0.99
H_1C_1	2.27	2.31	2.26			2.19
H_1C_2	2.26	2.16	2.19			2.21
C_1C_2	1.34	1.34	1.34			1.34
C_1C_3	3.90	4.22	4.23			4.18
C_1C_4	4.13	3.92	3.94			4.01
C_2C_3	4.24	5.13	5.24			4.80
C_2C_4	4.81	4.53	4.69			4.72
C_3C_4	1.33	1.34	1.34			1.34
AlC_1	4.51	4.36	4.22			4.24
AlC_2	4.65	4.61	4.64			4.70
AlC_3	4.56	5.24	5.24			5.50
AlC_4	5.12	4.66	4.66			6.22
transition states						
$O_{z1}H_1$	1.60	1.54	1.54	1.63	1.80	1.87
H_1C_1	1.20	1.23	1.24	1.94	1.99	1.90
H_1C_2	1.93	1.89	1.88	1.19	1.14	1.14
C_1C_2	1.41	1.41	1.40	1.42	1.44	1.45
C_2C_3	2.51	2.66	2.67	3.56	3.32	3.59
C_2C_4	2.53	2.50	2.51	3.39	3.31	3.16
C_1C_3	3.33	3.42	3.44	2.90	2.86	2.64
C_1C_4	3.29	3.28	3.29	2.78	2.58	2.62
C_3C_4	1.35	1.35	1.35	1.35	1.35	1.35
AlC_1	3.48	3.50	3.51	3.63	3.63	3.58
AlC_2	3.58	3.62	3.62	3.52	3.67	3.79
AlC_3	4.95	4.90	4.93	4.98	6.34	5.56
AlC_4	5.72	5.59	5.62	5.69	5.66	6.01
$O_{z2}H_2$	2.03	2.11	2.11	2.07	2.22	2.18
$O_{z2}H_1C_2$	150	151	151	145	117	124
dihedral-C_1[d]				173	171	170
dihedral-C_2[d]	172	173	173			

[a] Atom labels defined in Figure 4; distances in Å, angles in degrees. [b] Formally primary carbenium ion in the transition state; the charge is located on C_2. [c] Formally secondary carbenium ion in the transition state; the charge is located on C_1. [d] These are the dihedral angles formed by C_1/C_2 and the three substituents on these carbons, indicating the deviation from planarity (180°) around the carbon formally bearing the positive charge in the transition state.

of the second double bond, indicated by the almost equal distances from C_2 (primary) or C_1 (secondary) to C_3 and C_4 found in Table 6. This characteristic was also observed in the second transition state of the stepwise mechanism. Arstad et al.[20] have very recently published a theoretical cluster study on zeolite-catalyzed arene alkylation via a mechanism analogous to the concerted mechanism described here, and no such three-ring arrangement was found in the alkylation transition states in that case. It therefore seems that this feature is unique to reactions involving localized double bonds.

3.3. Stepwise versus Concerted Dimerization. Any attempts to extract quantitative information based on the current set of calculations warrant an initial discussion of the limitations inherent to the selected cluster model. There are two shortcomings that require particular attention. First, due to the limited size of the model surface, combined with our relying mainly on DFT methods, the strengths of *weak (dispersive) interactions* will be underestimated.[32] This causes, for instance, the energy differences between R1 and $R2_c$ and also $P1_s$ and $R2_s$ (see Figure 1) to become unrealistically small. However, this effect is expected to be fairly similar for all adsorbed states, thus becoming evened out when comparing the two mechanism types. Second, the omission of the major part of the zeolite wall in relatively close proximity to the active site might underestimate the effects of *steric limitations* related to the pore wall curvature or any other geometric peculiarity. Despite these drawbacks of the selected model, one aim of the present study was to decide which is the prevailing dimerization mechanism. Unfortunately, this effort was less conclusive than originally desired. The first barrier of the stepwise mechanism is always lower than the single barrier of the concerted pathway, whereas the second barrier of the stepwise mechanism is considerably higher than that of the concerted route. With this in mind, one could argue that concerted dimerization will dominate. However, if the chemisorption reaction, for which the lowest barrier is found, is driven to completion in the sense that every acidic site is occupied by an alkoxide, the concerted route becomes blocked.

The potential energy surfaces for both mechanisms are described graphically in Figure 1 and numerically in Tables 2 and 5. Strikingly, the highest-lying points on the PES are found for the concerted mechanism. Further, the energy differences between the topmost points for the two mechanisms are considerably smaller than the differences in activation barriers. On the basis of these observations, one could argue that the main cause of the high barrier found for the second step of the stepwise mechanism is the exothermicity of the alkoxide formation rather than an intrinsic instability of the second transition state as such. Simply put, after having formed the alkoxide, one appears to be positioned in an energy well, from which further progress of reaction requires the overcoming of a fairly high barrier. Thus, the relative energies of the physisorbed and chemisorbed alkenes ($\Delta E(\pi-\sigma)$) should be subjected to further scrutiny, as this issue appears to be decisive when it comes to discrimination between the two reaction mechanisms. We speculate that the predicted stability of the alkoxides may be related to an incomplete description of steric effects. A proper inclusion of these catalyst properties would

probably destabilize the alkoxides, which are covalently bound quite closely to the surface and thus very sensitive to the surface structure. The physisorbed alkenes are located farther from the zeolite surface and also exhibit greater mobility and will very likely adopt reasonably stable positions regardless of the geometric specifics. Some data supporting this view can be found in the literature. Most quantum chemical investigations on the alkoxide chemisorption (even those in which geometrically constrained clusters have been employed) do conclude that the reaction is exothermic,[17,25−30] as has also been found in the present study. There are, however, a few interesting exceptions. Boronat et al.[24,31] have combined cluster with periodic calculations specific to the structure of zeolite theta-1 and found the reaction to be endothermic, by as much as 60 kJ/mol, depending on alkene and calculation methodology. Rozanska et al.[34] have used periodic methods and found that steric constraints are very important with respect to the energetics of isobutene adsorption, and that the relative stabilities of *tert*-butoxide and a free *tert*-butyl carbenium ion critically depend on zeolite catalyst structure. In conclusion, we identify the alkene chemisorption step as a key reaction in determining which is the dominating mechanism. Further work, based on the qualitative description of alkene dimerization presented here, is necessary before this issue can be undisputedly settled.

Some experimental reports focusing on the mechanism of alkene dimerization can be found in the literature. Zecchina and co-workers[35,36] have studied the dimerization of ethene and propene over H−mordenite and H−ZSM-5 using IR spectroscopy. A stepwise mechanism was assumed, and this allowed the observations made to be satisfactory explained. However, monomeric alkoxide species were not specifically observed prior to dimer/oligomer formation, and a concerted mechanism was not discussed. Haw et al.[37] probed the oligomerization of propene over HY catalysts using in situ NMR spectroscopy and did indeed observe sec-propoxide species. Domen and co-workers[38,39] have used IR spectroscopy to investigate iso-butene oligomerization (which has not been studied here, but is considered relevant). Also in this case a monomeric alkoxide intermediate was assumed, but could not be observed. However, Trombetta et al.[40] did observe *tert*-butoxide groups during iso-butene oligomerization over H−ZSM-5 at low temperatures, but no alkoxides were observed when 1-butene or *trans*-2-butene were investigated. The fairly high reactivity of the intermediate alkoxide groups indicated by these experimental studies tends to contradict the quantum chemical predictions presented here, where the barrier for further reaction of the alkoxides are quite high. This further emphasizes the need for a better understanding of the stabilities of the alkoxides, to establish the depth of the energy well, if any, in which these species are located on the PES. Of course, the difficulties in observing the monomeric alkoxides are in accord with the concerted mechanism, for which no such intermediate is necessary.

3.4. β-Scission. Because of the incomplete description of the PES prior to product desorption from the catalyst surface after dimerization, only some information can be derived for the reverse reaction, the β-scission reaction. It is possible to assess the barriers for cracking of the alkenes listed in Table 1 by evaluating the energy differences between the dimerization products (as π- or σ-complexes) and the transition state of either mechanism. This information can be extracted from Tables 2 and 5, and when doing so the following observations can be made. (i) Since the dimerization reactions are exothermic, the barriers for β-scission are quite high. (ii) Cracking via the concerted mechanism and formally primary carbenium ions are highest for 1-butene and almost identical for 2-hexene and 3-octene. (iii) The concerted transition states involving primary carbenium ions are always higher in energy than those involving secondary ions. (iv) The order of reactivity for the remaining alkenes are 3,4-dimethyl-2-hexene > 5-methyl-3-heptene > 4-methyl-2-pentene > 1-butene, irrespective of reaction mechanism. (v) This holds both when the π- and σ-complexes are considered to be the reactant and at every level of theory employed.

4. Conclusions

The dimerization of ethene, propene, 1-butene, and *trans*-2-butene has been modeled using quantum chemical methods. Both concerted (simultaneous protonation and C−C bond formation) and stepwise (via alkoxides) dimerization have been evaluated. Formation of alkoxides, i.e., alkene chemisorption, has the lowest activation barrier of the investigated reaction steps. The barrier of the second step of the stepwise mechanism, the C−C bond formation step, has a higher activation energy than the single barrier of the concerted mechanism. For concerted dimerization via transition states resembling formally primary carbenium ions, the following order of reactivity has been found: *trans*-2-butene > 1-butene ≥ propene > ethene. Somewhat unexpectedly, the opposite order of reactivity is predicted for concerted dimerization via formally secondary carbenium ion-like transition states: propene ≥ 1-butene > *trans*-2-butene. The stepwise mechanism, where only the most stable transition states (secondary) were investigated, resulted in the following ordering: 1-butene ≥ *trans*-2-butene > propene > ethene. Attempts to determine which is the prevailing reaction mechanism have been inconclusive. More detailed knowledge concerning the stability of alkoxide species relative to physisorbed alkenes will be necessary for discrimination between the two mechanistic proposals.

Acknowledgment. Thanks are due to the Norwegian Research Council for a grant of computer time through the NOTUR project (accounts NN2878K and NN2147K).

Supporting Information Available: Cartesian coordinates and absolute energies for all stationary points. Pictures of some transition states with displacement vectors. This material is available free of charge via the Internet at http://pubs.acs.org.

References and Notes

(1) O'Connor, C. T.; Kojima, M. *Catal. Today* **1990**, *6*, 329−349.
(2) Golombok, M.; de Bruijn, J. *Ind. Eng. Chem. Res.* **2000**, *39*, 267−271.
(3) Schmerling, L.; Ipatieff, V. N. *Adv. Catal.* **1950**, *2*, 21−78.
(4) Gigstad, I.; Kolboe, S. Propene Oligomerization over Dealuminated Mordenite. In *Progress in Zeolite and Microporous Materials*; Chon, H., Ihm, S.-K., Uh, Y. S., Eds.; Stud. Surf. Sci. Catal. 105; Elsevier Science: Amsterdam, 1997; 965−972.
(5) Knifton, J. F.; Sanderson, J. R.; Dai, P. E. *Catal. Lett.* **1994**, *28*, 223−230.
(6) Hsia Chen, C. S.; Bridger, R. F. *J. Catal.* **1996**, *161*, 687−693.
(7) van Niekerk M. J.; O'Connor, C. T.; Fletcher, J. C. Q. *Ind. Eng. Chem. Res.* **1996**, *35*, 697−702.
(8) Quann, R. J.; Green, L. A.; Tabak, S. A.; Krambeck, F. J. *Ind. Eng. Chem. Res.* **1988**, *27*, 565−570.
(9) Kojima, M.; Rautenbach, M. W.; O'Connor, C. T. *Ind. Eng. Chem. Res.* **1988**, *27*, 248−252.
(10) Stöcker, M. *Microporous Mesoporous Mater.* **1999**, *29*, 3−48.
(11) Svelle, S.; Arstad, B.; Kolboe, S.; Swang, O. *J. Phys. Chem. B* **2003**, *107*, 9281−9289.
(12) Hay, P. J.; Redondo, A.; Guo, Y. *Catal. Today* **1999**, *50*, 517−523.
(13) Frash, M. V.; Kazansky, V. B.; Rigby, A. M.; van Santen, R. A. *J. Phys. Chem. B.* **1998**, *102*, 2232−2238.

(14) Rigby, A. M.; Kramer, G. J.; van Santen, R. A. *J. Catal.* **1997**, *170*, 1−10.
(15) Kazansky, V. B. *Catal. Today* **1999**, *51*, 419−434.
(16) Frash, M. V.; van Santen, R. A. *Top. Catal.* **1999**, *9*, 191−205.
(17) Sinclair, P. E.; de Vries, A.; Sherwood, P.; Catlow, C. R. A.; van Santen, R. A. *J. Chem. Soc., Faraday Trans.* **1998**, *94*, 3401−3408.
(18) Arstad, B.; Kolboe, S.; Swang, O. *J. Phys. Chem. B* **2002**, *106*, 12722−12726.
(19) Svelle, S.; Kolboe, S.; Swang, O. *J. Phys. Chem. B* **2003**, *107*, 5251−5260.
(20) Arstad, B.; Kolboe, S.; Swang, O. *J. Phys. Chem. B*, accepted for publication.
(21) Rozanska, X.; Saintigny, X.; van Santen, R. A.; Hutschka, F. *J. Catal.* **2001**, *202*, 141−155.
(22) Rozanska, X.; van Santen, R. A.; Hutschka, F.; Hafner, J. *J. Am. Chem. Soc.* **2001**, *123*, 7655−7667.
(23) Frisch, M. J.; Trucks, G. W.; Schlegel, H. B.; Scuseria, M. A.; Robb, M. A.; Cheeseman, J. R.; Zakrzewski, V. G.; Montgomery, J. A.; Stratmann, R. E.; Burant, J. C.; Dapprich, S.; Millam, J. M.; Daniels, A. D.; Kudin, K. N.; Strain, M. C.; Farkas, O.; Tomasi, J.; Barone, V.; Cossi, M., Cammi, R.; Mennucci, B.; Pomelli, C.; Adamo, C.; Clifford, S.; Ochterski, J.; Petersson, G. A.; Ayala, P. Y.; Cui, Q.; Morokuma, K.; Malick, D. K.; Rabuck, D. K.; Raghavachari, K.; Foresman, J. B.; Cioslowski, J.; Ortiz, J. V.; Stefanov, B. B.; Liu, G.; Liashenko, A.; Piskorz, P.; Komaromi, I.; Gomperts, R.; Martin, R. L.; Fox, D. J.; Keith, T.; Al-Laham, M. A.; Peng, C. Y.; Nanayakkara, A.; Gonzales, C.; Challacombe, M.; Gill, P. M. W.; Johnson, B. G.; Chen, W.; Wong, M. W.; Andres, J. L.; Head-Gordon, M.; Replogle, E. S.; Pople, J. A. *Gaussian98*, revision A.11; Gaussian, Inc.: Pittsburgh, PA, 1998.
(24) Boronat, M.; Zicovich-Wilson, C. M.; Viruela, P.; Corma, A. *J. Phys. Chem. B* **2001**, *105*, 11169−11177.
(25) Correa, R. J.; Mota, C. J. A. *Phys. Chem. Chem. Phys.* **2002**, *4*, 375−380.
(26) Evleth, E. M.; Kassab, E.; Jessri, H.; Allavena, M.; Montero, L.; Sierra, L. R. *J. Phys. Chem. B* **1996**, *100*, 11368−11374.
(27) Viruela-Martín, P.; Zicovich-Wilson, C. M.; Corma, A. *J. Phys. Chem. B* **1993**, *97*, 13713−13719.
(28) Boronat, M.; Viruela, P.; Corma, A. *J. Phys. Chem. A* **1998**, *102*, 982−989.
(29) Rigby, A. M.; Frash, M. V. *J. Mol. Catal. A* **1997**, *126*, 61−72.
(30) Kazansky, V. B.; Senchenya, I. N. *J. Catal.* **1989**, *119*, 108−120.
(31) Boronat, M.; Zicovich-Wilson, C. M.; Viruela, P.; Corma, A. *Chem. Eur. J.* **2001**, *7*, 1295−1303.
(32) Sauer, J.; Ugliengo, P.; Garrone, E.; Saunders: V. R. *Chem. Rev.* **1994**, *94*, 2095−2160.
(33) (a) Brønsted, N. *Chem. Rev.* **1928**, *5*, 231−338. (b) Evans, M. G.; Polanyi, N. P. *Trans. Faraday Soc.* **1938**, *34*, 11−29.
(34) Rozanska, X.; van Santen, R. A.; Demuth, T.; Hutschka, F.; Hafner, J. *J. Phys. Chem. B* **2003**, *107*, 1309−1315.
(35) Spoto, G.; Bordiga, S.; Ricchiardi, G.; Scarano, D.; Zecchina, A.; Borello, E. *J. Chem. Soc., Faraday Trans.* **1994**, *90*, 2827−2835.
(36) Geobaldo, F.; Spoto, G.; Bordiga, S.; Lamberti, C.; Zecchina, A. *J. Chem. Soc., Faraday Trans.* **1997**, *93*, 1243−1249.
(37) Haw, J. F.; Richardson, B. R.; Oshiro, I. S.; Lazo, N. D.; Speed, J. A. *J. Am. Chem. Soc.* **1989**, *111*, 2052−2058.
(38) Ishikawa, H.; Yoda, E.; Kondo, J. N.; Wakabayashi, F.; Domen, K. *J. Phys. Chem. B* **1999**, *103*, 5681−5686.
(39) Kondo, J. N.; Ishikawa, H.; Yoda, E.; Wakabayashi, F.; Domen, K. *J. Phys. Chem. B* **1999**, *103*, 8538−8543.
(40) Trombetta, M.; Busca, G.; Rossini, S.; Piccoli, V.; Cornaro, U. *J. Catal.* **1997**, *168*, 349−363.